

Effects on the structure of the universe of an accelerating expansion *

George A. Baker, Jr.

*Theoretical Division, Los Alamos National Laboratory
University of California, Los Alamos, N. M. 87544 USA*

535 May 7, 2019

Abstract. Recent experimental results from supernovae Ia observations have been interpreted to show that the rate of expansion of the universe is increasing. Other recent experimental results find strong indications that the universe is “flat.” In this paper, I investigate some solutions of Einstein’s field equations which go smoothly between Schwarzschild’s relativistic gravitational solution near a mass concentration to the Friedmann-Lemaître expanding universe solution. In particular, the static, *curved-space extension* of the Lemaître-Schwarzschild solution in vacuum is given. Uniqueness conditions are discussed. One of these metrics preserves the “cosmological equation.” We find that when the rate of expansion of the universe is increasing, space is broken up into domains of attraction. Outside a domain of attraction, the expansion of the universe is strong enough to accelerate a test particle away from the domain boundary. I give a *domain-size-mass relationship*. This relationship may very well be important to our understanding of the large scale structure of the universe.

pacs: 96.30Sf, 97.60Bw, 95.85Bh, 04.20-q

1. INTRODUCTION AND SUMMARY

Recently de Bernardis *et al.*[1] reported that a very careful examination of the cosmic microwave background provides, as further explained by Hu[2], very strong evidence that the universe is flat!

In addition, data has recently been reported by Riess *et al.*[3], and Perlmutter *et al.*[4] on measurements of the luminosity and the redshift of a number of high-redshift supernovae of type Ia. The authors’ best fit to their data involves a strongly curved space-time. The curvature constant Ω_k (defined below) that they find is about -1.05, which corresponds to a strongly curved, open universe. However, their error bars are sufficiently large so that a flat universe is not inconsistent with their data. These authors have analyzed their data on the basis of the “cosmological equation” between the rate of expansion, the mean energy density, the radius of curvature of space, and the cosmological constant. This relation has been derived from Einstein’s field equations[5] under the assumption of the validity of the Friedmann-Lemaître line

* Work supported in part by the US Department of Energy (contract W-7405-ENG-36)



element at large distances. The authors have concluded, in terms of this model of the universe, that instead of the rate of expansion decreasing, as many workers had thought, their data is best fit by a model in which the rate of expansion is increasing. Riess *et al.*[3] find that the deceleration/acceleration parameter (as defined in section VI) $q_0 < 0$ (acceleration) with better than 90% confidence, and Perlmutter *et al.*[4] find the same at the 2.86 standard deviation level of confidence.

In this paper, I investigate some different metrics which may facilitate the investigation of some of the consequences of the reported acceleration of the expansion of the universe. I will focus on spherically symmetric models with a central mass concentration.

The fact that the rate of expansion of the universe is increasing leads to the conclusion that the universe is broken up into domains of attraction. Briefly, the underlying physics of this feature may be seen in the following rough analysis. The equation of purely radial motion of a test particle at rest with respect to the Friedmann-Lemaître coordinate system is just

$$\ddot{r} = \frac{\ddot{a}}{a}r, \quad (1)$$

where r is the proper distance, and a is the universal expansion factor which is a function of time alone. The most simple way to approximate the effects of a gravitating mass concentration is just to add Newton's force term so that

$$\ddot{r} = \frac{\ddot{a}}{a}r - \frac{GM}{r^2}. \quad (2)$$

If the expansion of the universe is decelerating, then $\ddot{a} < 0$, so $\ddot{r} < 0$ always. Near a gravitating mass the expansion is clearly unimportant and Newton's laws hold with only minimal corrections. On the other hand, if the expansion is accelerating, then $\ddot{a} > 0$. Thus there will be a distance such that the expansion of the universe exactly balances the gravitational attraction. Test particles at smaller distances will be accelerated inwards. I call this region a domain of attraction. Test particles outside will be accelerated outwards. Hence in this very simple case there are two attractors, one is the mass concentration and the other is the point at infinity. We give a *domain-size-mass relation* in equations (73) and (76). In the decelerating case, there is just one attractor and its domain of attraction is the entire space.

In the second section we remind the reader of the Lemaître-Tolman formalism. This formalism has the feature that the proper time appears explicitly. Thus space-time is divided into a set of three-dimensional, space-like manifolds which are indexed by the proper time. Since it is the proper time which appears in the universal expansion function in the Friedmann-Lemaître line element and it governs the universe as a

whole, it seems important to preserve the property that the universal expansion factor is a function of the proper time alone.

In the third section we review three different ways to go from the Schwarzschild metric of a planetary system to expanding space at large distances. The McVittie solution has a problem at the Schwarzschild radius using normal expansion factors. The Einstein-Straus “Swiss Cheese Model” is unstable to perturbations and there are orbits which are discontinuous functions of their initial conditions. The Bona-Stela model using Liebovitz metric insertions in a Friedmann-Lemaître background predicts an increase in the length of the earth’s year which is in strong disagreement with observations.

In the fourth section we consider the idea that the vacuum is something more than just empty space. The self-energy of the vacuum may correspond to a mass-energy density of empty space. We know on the laboratory scale from, for example, the Casimir effect, and on the microscopic scale from particle physics that the vacuum does have measurable effects. So far as I know, particle theorists have not yet been able to compute a quantitative result for the energy density. However, they do feel that such an idea is extremely plausible. We consider in this section a solution to Einstein’s field equations which has a homogeneous vacuum, mass-energy density and so preserves the so called “cosmological equation.” This solution reduces precisely to the exterior Schwarzschild solution near the central mass condensation. In addition, it reduces to the Friedmann-Lemaître solution far from the mass concentration. This solution is continuously, infinitely differentiable everywhere, except at the mass concentration.

In the fifth section, I explore some of the properties of the solution obtained in the fourth section. Both “flat” and curved space are considered. The limiting results are as expected and the transition between the two aforementioned limits are illustrated. In particular the static, *curved-space extension* of the Lemaître-Schwarzschild solution is given for a mass concentration in a vacuum.

In the sixth section, I consider the implications of the increasing rate of expansion of the universe on some of the large scale structures found in the universe. It is found that this feature creates domains of attraction. A *domain-size-mass relation* is derived. Outside these domains, the increasing rate of the expansion of the universe would, in time, be expected to tear the structures apart. It is suggested, from the correspondence between the predicted size of these domains of attraction, the size of the Local Group, and the size of the Virgo Cluster, that this effect may well be important in any study of the large scale structure of the universe.

2. THE LEMAÎTRE-TOLMAN FORMALISM

I will find it convenient to employ the Lemaître-Tolman[6, 7] formalism. In this case we start with the line element,

$$ds^2 = -e^{2\alpha(\rho,\tau)}d\rho^2 - e^{2\beta(\rho,\tau)}(d\theta^2 + \sin^2\theta d\phi^2) + c^2d\tau^2, \quad (3)$$

where c is the velocity of light, and τ is the proper time for an observer at rest in this coordinate system. This line element is spherically symmetric in its structure, which is of sufficient generality for my purposes.

The reason for our interest in this particular form of the line element is that two important line elements are special cases. First, the Friedmann-Lemaître line element,

$$ds^2 = -a^2(\tau)d\rho^2 - a^2(\tau)\rho^2(d\theta^2 + \sin^2\theta d\phi^2) + c^2d\tau^2 \quad (4)$$

is manifestly of form (3). The second important line element is the static Schwarzschild line element. It is usually written in the form,

$$ds^2 = -\frac{dr^2}{1 - \frac{2GM}{c^2r}} - r^2(d\theta^2 + \sin^2\theta d\phi^2) + c^2\left(1 - \frac{2GM}{c^2r}\right)dt^2 \quad (5)$$

However, as is well known[8] this form does not extend inside the Schwarzschild radius $r_S = 2GM/c^2$. An alternate form has been given by Lemaître [9]. It is

$$ds^2 = -\frac{2GM}{c^2\mathcal{R}}d\rho^2 - \mathcal{R}^2(d\theta^2 + \sin^2\theta d\phi^2) + c^2d\tau^2, \\ \mathcal{R} \equiv \left[\frac{3}{2}\sqrt{2GM/c^2}(\rho - c\tau)\right]^{2/3}. \quad (6)$$

This form, without going into the full generality of the Schwarzschild solution, has no singularity at the Schwarzschild radius. It is a coordinate system adapted to a freely falling observer. This metric can easily be seen to have the form (3). As it is our goal to find a metric which tends asymptotically to the Friedmann-Lemaître metric at very large distances, and tends asymptotically to the Schwarzschild metric on the scale of our planetary system, it seems appropriate to use the Lemaître-Tolman formalism. In this formalism, four dimensional space-time is described by a set of three-dimensional, space-like hypersurfaces, indexed by the time like variable τ .

Next we consider the stress-energy tensor for the line element (3). First,

$$8\pi cT_1^4 = -2\left(\beta'\dot{\beta} - \dot{\alpha}\beta' + \dot{\beta}'\right) = 0, \quad (7)$$

where an overdot means differentiation with respect to τ and $'$ means differentiation with respect to ρ . The conditions $T_1^4 = -e^{2\alpha}T_4^1 = 0$ are set in order to have a time-orthogonal coordinate system. The solution of this equation is well known to be,

$$e^\alpha = \frac{\beta' e^\beta}{f(\rho)}, \quad 0 < f(\rho) < \infty, \quad (8)$$

where $f(\rho)$ is undetermined. This result allows us to eliminate $\alpha(\rho, \tau)$ in terms of $\beta(\rho, \tau)$ and $f(\rho)$.

The other non-zero elements of the stress-energy tensor are,

$$\begin{aligned} 8\pi T_1^1 &= e^{-2\beta} - e^{-2\alpha}(\beta')^2 + 2\frac{\ddot{\beta}}{c^2} + 3\left(\frac{\dot{\beta}}{c}\right)^2 - \Lambda \\ &= 2\frac{\ddot{\beta}}{c^2} + 3\left(\frac{\dot{\beta}}{c}\right)^2 + e^{-2\beta}[1 - f^2(\rho)] - \Lambda \end{aligned} \quad (9)$$

$$\begin{aligned} 8\pi T_2^2 &= 8\pi T_3^3 = \frac{\ddot{\beta} + \dot{\beta}^2 + \dot{\alpha}\dot{\beta} + \ddot{\alpha} + \dot{\alpha}^2}{c^2} - e^{-2\alpha}[\beta'' + (\beta')^2 - \alpha'\beta'] - \Lambda \\ &= 8\pi T_1^1 + \frac{8\pi}{2\beta'} \frac{\partial T_1^1}{\partial \rho} \end{aligned} \quad (10)$$

$$\begin{aligned} 8\pi T_4^4 &= \left(\frac{\dot{\beta}}{c}\right)^2 + 2\frac{\dot{\alpha}\dot{\beta}}{c^2} + e^{-2\beta} - e^{-2\alpha}[2\beta'' + 3(\beta')^2 - 2\alpha'\beta'] - \Lambda \\ &= 3\left(\frac{\dot{\beta}}{c}\right)^2 + 2\frac{\dot{\beta}\dot{\beta}'}{c^2\beta'} + e^{-2\beta} \left[1 - f^2(\rho) - \frac{2f(\rho)f'(\rho)}{\beta'}\right] - \Lambda \end{aligned} \quad (11)$$

We see that by (10), the necessary and sufficient condition that the spatial curvature be isotropic is that T_1^1 be independent of ρ . In addition, this condition implies that the spatial curvature is homogeneous throughout all space.

If we replace $f(\rho)$ by unity, then by construction, $e^\beta = \int e^\alpha d\rho$, the distance measured from the origin. Hence the area of a sphere is just 4π times the square of the radius, as is given by the standard Euclidean formula. I will call this special case the case of “flat” space. In the special case of “flat” space and isotropic spatial curvature, (9) and (11) become

$$8\pi T_1^1 = 8\pi T_2^2 = 8\pi T_3^3 = 2\frac{\ddot{\beta}}{c^2} + 3\left(\frac{\dot{\beta}}{c}\right)^2 - \Lambda, \quad (12)$$

$$8\pi T_4^4 = \frac{\dot{\beta}}{c} \left(3\frac{\dot{\beta}}{c} + 2\frac{\dot{\beta}'}{c\beta'}\right) - \Lambda. \quad (13)$$

We observe, that (9) and (11) may be rewritten as,

$$\frac{\partial}{\partial \tau} \left\{ e^{3\beta} \left[\left(\frac{\dot{\beta}}{c} \right)^2 - \frac{\Lambda}{3} \right] + e^\beta [1 - f^2(\rho)] \right\} = 8\pi T_1^1 \dot{\beta} e^{3\beta} \quad (14)$$

$$\frac{\partial}{\partial \rho} \left\{ e^{3\beta} \left[\left(\frac{\dot{\beta}}{c} \right)^2 - \frac{\Lambda}{3} \right] + e^\beta [1 - f^2(\rho)] \right\} = 8\pi T_4^4 \beta' e^{3\beta}. \quad (15)$$

The quantity

$$m = \frac{c^2}{2G} \left\{ e^{3\beta} \left[\left(\frac{\dot{\beta}}{c} \right)^2 - \frac{\Lambda}{3} \right] + e^\beta [1 - f^2(\rho)] \right\} \quad (16)$$

is easily recognized[6, 10] to be the mass equivalent to the total energy contained within the comoving shell with radial coordinate ρ at time τ .

We will also be concerned with the dynamics as seen in this formalism. The main interest will be to assess the difference between the effects on planetary systems of the metrics which we will study herein, and the Schwarzschild metric. In particular I am interested in the solar system. The standard formula for the equations of motion of a test particle[5] is

$$\left(\frac{ds}{d\tau} \right) \frac{d}{d\tau} \left[g_{ki} \left(\frac{ds}{d\tau} \right)^{-1} \dot{x}^i \right] = \frac{1}{2} g_{ij,k} \frac{dx^i}{d\tau} \frac{dx^j}{d\tau} \quad (17)$$

where of course $dx^4/d\tau = 1$. The fourth component of (17) gives the convenient equation,

$$\mathcal{B} = \left(\frac{ds}{d\tau} \right) \frac{d}{d\tau} \left[\left(\frac{ds}{d\tau} \right)^{-1} \right] = - \left\{ \frac{\dot{\alpha} e^{2\alpha} \dot{\rho}^2 + \dot{\beta} e^{2\beta} [\dot{\theta}^2 + \sin^2 \theta \dot{\phi}^2]}{c^2} \right\} \quad (18)$$

Explicitly, the three equations of motion are,

$$\mathcal{B} e^{2\alpha} \dot{\rho} + \frac{d}{d\tau} [e^{2\alpha} \dot{\rho}] = \alpha' e^{2\alpha} \dot{\rho}^2 + \beta' e^{2\beta} [\dot{\theta}^2 + \sin^2 \theta \dot{\phi}^2], \quad (19)$$

$$\mathcal{B} e^{2\beta} \dot{\theta} + \frac{d}{d\tau} [e^{2\beta} \dot{\theta}] = e^{2\beta} \sin \theta \cos \theta \dot{\phi}^2, \quad (20)$$

$$\left(\frac{ds}{d\tau} \right) \frac{d}{d\tau} \left[e^{2\beta} \sin^2 \theta \left(\frac{ds}{d\tau} \right)^{-1} \dot{\phi} \right] = 0. \quad (21)$$

Following the completely standard *modus operandi*, we make an immediate simplification by setting $\theta = \pi/2$. Now equation (20) is explicitly satisfied and the other two equations are simplified. The first integral of (21) gives us the conservation of angular momentum, to wit,

$$e^{2\beta}\dot{\phi} = C_0 \left(\frac{ds}{d\tau} \right), \quad (22)$$

where the C_i are constants of integration. By means of (3) we may write (22) as,

$$\dot{\phi}^2 = C_0^2 e^{-4\beta} \left(c^2 - e^{2\alpha} \dot{\rho}^2 - e^{2\beta} \dot{\phi}^2 \right) = \frac{C_0^2 e^{-4\beta} (c^2 - e^{2\alpha} \dot{\rho}^2)}{1 + C_0^2 e^{-2\beta}}. \quad (23)$$

These steps leave us with the single equation (19) for $\rho(\tau)$ to deal with. It now becomes

$$\mathcal{B}\dot{\rho} + (2\dot{\alpha} + \alpha'\dot{\rho})\dot{\rho} + \ddot{\rho} = \frac{\dot{\phi}^2}{\beta'} = \frac{C_0^2 e^{-4\beta} (c^2 - e^{2\alpha} \dot{\rho}^2)}{\beta' (1 + C_0^2 e^{-2\beta})}, \quad (24)$$

where \mathcal{B} (18) may be re-expressed as,

$$\mathcal{B} = -\dot{\alpha} e^{2\alpha} \left(\frac{\dot{\rho}}{c} \right)^2 - \frac{C_0^2 \dot{\beta} e^{-2\beta} (c^2 - e^{2\alpha} \dot{\rho}^2)}{c^2 (1 + C_0^2 e^{-2\beta})} \quad (25)$$

Thus, (19) becomes,

$$\ddot{\rho} = -(2\dot{\alpha} + \alpha'\dot{\rho})\dot{\rho} + \frac{C_0^2 e^{-2\beta} (c^2 e^{-2\beta} + \dot{\beta}\beta'\dot{\rho}) (c^2 - e^{2\alpha} \dot{\rho}^2)}{c^2 \beta' (1 + C_0^2 e^{-2\beta})} + \dot{\rho} \dot{\alpha} e^{2\alpha} \left(\frac{\dot{\rho}}{c} \right)^2 \quad (26)$$

which gives an explicit, ordinary, non-linear differential equation for $\rho(\tau)$. Coupled with $\theta = \pi/2$ and equation (23), we have the equations of motion of the test particle.

A more transparent form follows for the purpose of identifying the corrections to the Schwarzschild dynamics results if we make the change of variables,

$$r = \exp[\beta(\rho, \tau)], \quad \Rightarrow \quad \rho = \rho(r, \tau). \quad (27)$$

Then we have

$$\dot{r} = (\dot{\beta} + \beta'\dot{\rho}) r. \quad (28)$$

Equation (19) becomes,

$$\ddot{r} = \left[\ddot{\beta} + \dot{\beta}^2 + \frac{f'}{f\beta'} \left(\frac{\dot{r}}{r} - \dot{\beta} \right)^2 \right] r + \frac{c^2 C_0^2}{r^3} + \left(\frac{\dot{\beta}' + \dot{\beta}\beta'}{c^2 f^2 \beta'} \right) (\dot{r} - r\dot{\beta})^3$$

$$+ \frac{C_0^2 \left[\frac{\dot{\beta}}{r}(\dot{r} - \dot{\beta}r) - \left(\frac{\dot{r} - \dot{\beta}r}{rf} \right)^2 - \frac{\dot{\beta}(\dot{r} - \dot{\beta}r)^3}{rc^2f^2} - \frac{C_0^2c^2}{r^4} \right]}{r(1 + C_0^2/r^2)}. \quad (29)$$

3. CLASSICAL MODELS

Currently there are two general relativistic descriptions of spacetime in popular use. For planetary systems and other gravitationally bound structures which are small on the scale of the universe, there is a static description of the behavior of spacetime. On the other hand, for large-scale behavior, there is a time dependent description which is appropriate as a description of phenomena such as the observed red-shift of distant galaxies.

The classic question is, ‘‘How can these two disparate descriptions of spacetime possibly be reconciled with each other?’’ The first answer to this problem was given by McVittie[11]. Using the line element form,

$$ds^2 = -e^\mu(d\rho^2 + \rho^2d\theta^2 + \rho^2\sin^2\theta d\phi^2) + e^\nu dt^2 \quad (30)$$

He proposed the solution,

$$\begin{aligned} e^\mu &= \frac{a(t)^2}{[1 + (a(t)\rho/2a(t)R)^2]^2} \left(1 + \frac{m}{2a(t)\rho} \right)^4 \\ e^\nu &= c^2 \left(\frac{1 - m/2a(t)\rho}{1 + m/2a(t)\rho} \right)^2 \quad m \equiv \frac{GM}{c^2} \left[1 + \left(\frac{\rho}{2R} \right)^2 \right]^{1/2} \end{aligned} \quad (31)$$

where G is Newton’s constant of gravitation. Some of the virtues of this model can be seen by examining the corresponding stress-energy tensor,

$$\begin{aligned} 8\pi T_1^1 &= \frac{1 + (m/2a(t)\rho)^2}{a(t)^2 R^2 (1 + m/2a\rho)^5 (1 - m/2a(t)\rho)} \\ &\quad + \frac{2\ddot{a}a[1 + m/2a(t)\rho] + \dot{a}^2[1 - 5m/2a(t)\rho]}{a(t)^2 c^2 (1 - m/2a(t)\rho)} - \Lambda \\ 8\pi T_2^2 &= 8\pi T_3^3 = 8\pi T_1^1 \\ 8\pi T_4^4 &= \frac{3}{a(t)^2 R^2 (1 + m/2a(t)\rho)^5} + \frac{3\dot{a}^2}{c^2 a^2} - \Lambda. \end{aligned} \quad (32)$$

In the limit as $m \rightarrow 0$ or $\rho \rightarrow \infty$ these tensor elements reduce to those corresponding to (4), and also in the limit as $R \rightarrow \infty$ and $\dot{a} \rightarrow 0$ they

vanish as with the Schwarzschild metric. For this metric the spatial curvature is isotropic, but not homogeneous. The dynamical behavior of a test particle can be computed from (17). In the usual case $\theta = \pi/2$, the equation of motion, analogous to (29), becomes,

$$\begin{aligned} & \ddot{r} - 2\frac{\dot{a}}{a}\dot{r} + r \left[2\left(\frac{\dot{a}}{a}\right)^2 - \frac{\ddot{a}}{a} \right] + \dot{\mu} \left(\dot{r} - \frac{\dot{a}}{a}r \right) \\ &= \frac{1}{2}\mu'a \left(\frac{\dot{r}}{a} - \frac{\dot{a}}{a^2}r \right)^2 + \frac{1}{2} \left(\mu'\frac{r}{a} + 2 \right) \left[\frac{A^2 a^4 e^{-2\mu}}{r^3} \right] \left(\frac{ds}{dt} \right)^2 \\ & \quad - \frac{1}{2}\nu'ae^{\nu-\mu} - \frac{1}{2} \left(\frac{ds}{dt} \right)^2 \frac{d}{dt} \left[\left(\frac{ds}{dt} \right)^{-2} \right] \left(\dot{r} - \frac{\dot{a}}{a}r \right), \end{aligned} \quad (33)$$

where, in concert with (22), $r^2 e^\mu \dot{\phi} = A(ds/dt)$, and the change of variables $r = a(t)\rho$ has been used. The slow speed limit of this equation of motion is,

$$\ddot{r} = \frac{\ddot{a}}{a}r + \frac{A^2 c^2}{r^3} - \frac{GM}{r^2} \quad (34)$$

This equation differs from Newton's by the \ddot{a} term. This term is proportion to H_0^2 where $H_0 \approx 1.62 \times 10^{-18} h_{50}$ is Hubble's constant. $h_{50} = 1$ if $H_0 = 50$ km/sec/Megaparsec. Thus in McVittie's model, the effects on the solar system are too small to be currently measured. For systems like the solar system, the McVittie model works very well. However for other systems, if we make the popular assumption that $a(t) \propto t^\gamma$ then, as in McVittie's solution $a(t)$ is a function of coordinate time and not of proper time, there will be a singularity at the the Schwarzschild radius as $a(t)$ will diverge there since $t \rightarrow \infty$.

A second answer to our question was given by Einstein and Straus [12]. It is the so called "Swiss Cheese Model." They showed that the static Schwarzschild metric (5) can be matched to any Friedmann-Lemaître-Robertson-Walker metric on a spherical surface of an expanding radius in the Schwarzschild metric, but of a constant radius in the Friedmann-Lemaître-Robertson-Walker metric. It has been found however[13, 14] to be unstable with respect to perturbations. In addition, there is another unphysical aspect of this model. The slow-speed dynamical equations in the interior Schwarzschild (\vec{r}_i) and in the exterior Friedmann-Lemaître (\vec{r}_e) regions are, respectively,

$$\frac{d^2 \vec{r}_i}{dt^2} = -\frac{GM}{r_i^3} \vec{r}_i, \quad \frac{d^2 \vec{r}_e}{dt^2} = \frac{\ddot{a}}{a} \vec{r}_e. \quad (35)$$

For ease of exposition, we choose $a(t) = (t/t_0)^{2/3}$. Thus the general solution in the exterior region is $\vec{r}_e = \vec{A}t^\gamma + \vec{B}t^{1-\gamma} = \vec{A}t^{2/3} + \vec{B}t^{1/3}$, which is the equation of a parabola.

As an illustration of the behavior of the ‘‘Swiss cheese model’’ I have computed the following trajectories. I use as a unit of time the Hubble time, that is $1/H_0$. As a unit of distance I use $\sqrt[3]{M_\odot G/H_0^2}$ which is about $25h_{50}^{-2/3}$ million Astronomical units. M_\odot is the mass of the Sun. I set $t_0 = 1$. The metric interface is at $r = t^{2/3}$ in these units for flat spacetime, as mentioned above. In order to follow a Friedmann-Lemaître trajectory the test particle’s distance from the origin must be larger at every time than that for the interface. Let us take in rectangular coordinates the initial conditions, $x = \lambda$, $\dot{x} = 0$, $y = 0$, $\dot{y} = \lambda$. The trajectory in the external region is

$$\begin{aligned} x &= \lambda \left[-\left(\frac{t}{t_0}\right)^{2/3} + 2\left(\frac{t}{t_0}\right)^{1/3} \right] \\ y &= 3t_0\lambda \left[\left(\frac{t}{t_0}\right)^{2/3} - \left(\frac{t}{t_0}\right)^{1/3} \right]. \end{aligned} \quad (36)$$

Thus,

$$\lambda^2 \left[10t^{4/3} - 22t + 13t^{2/3} \right] > t^{4/3}. \quad (37)$$

The trajectory will intersect the interface if equation (37) is an equality. By means of the quadratic formula, an intersection will occur if

$$t^{1/3} = \frac{11 \pm \sqrt{-9 + 13/\lambda^2}}{10 - 1/\lambda^2}. \quad (38)$$

It will be observed that for $\lambda < \sqrt{13}/3$ there are two real roots. If $\lambda = 1$, then $t^{1/3} = 1, 13/9$. On the other hand, if $\lambda > \sqrt{13}/3$, the roots are imaginary, so there are no intersections. If $\lambda = \sqrt{13}/3$ there is a double root at $t^{1/3} = 13/11$. In this case the parabolic trajectory just grazes the metric interface.

In figure 1, I illustrate the two different trajectories when $r_0 = \sqrt{13}/3$ and $\dot{\phi}_0 = 1.0$. In the case where r_0 is just any arbitrary amount smaller, the expanding interface overtakes the test particle following its Friedmann-Lemaître parabolic trajectory and it must then follow the static Schwarzschild equations of motion. The Schwarzschild metric takes over at $t = (13/11)^3$ as explained above, and after that the trajectory is an ellipse with semimajor axis 7.6287 and the semiminor axis 3.986. These imply an eccentricity of 0.69068 and a semilatus rectum parameter of $p = 2.086$. On the other hand, if r_0 is any arbitrary amount larger, it escapes the moving interface and continues to follow the parabolic trajectory. It is evident from figure 1 that future trajectories are, in some cases, discontinuous functions of the initial conditions for the ‘‘Swiss cheese model.’’

Put another way, the Schwarzschild metric permits closed orbits and the Friedmann-Lemaître metric does not. In terms of the latter coordinates, one can choose initial conditions so that the parabolic trajectory just grazes the metric interface (fixed radial coordinate in this metric) and the speed is low enough that for infinitesimally different initial conditions the trajectory crosses the interface and is caught in a bound state, or alternatively misses the interface and proceeds on its parabolic trajectory. All these effects take place in supposedly empty space of the order of $25h_{50}^{-2/3}$ million AU from a mass concentration of size M_{\odot} , and are quite counter to one's physical intuition that such discontinuities should not occur there, except perhaps if the central void was created by an explosion leaving a remnant star behind.

A third answer was provided by Bona and Stela[15]. It is a different type of "Swiss Cheese Model." They insert in a flat space, Friedmann-Lemaître-Robertson-Walker background a spherical patch in which, instead of the Schwarzschild metric, the Liebovitz[16] solution is inserted. In the classification of Krasiński[10], this solution is in the " $\beta' \neq 0$ " subfamily of the Szekeres-Szafron family of solutions. Briefly put, this solution results from setting T_1^1 equal to its Friedmann-Lemaître value, *i.e.*, by (9),

$$8\pi T_1^1 = 2\frac{\ddot{\beta}}{c^2} + 3\left(\frac{\dot{\beta}}{c}\right)^2 - \Lambda = 2\frac{\ddot{a}}{ac^2} + \left(\frac{\dot{a}}{ac}\right)^2 - \Lambda \quad (39)$$

Since the right hand side of (39) is independent of ρ , the spatial curvature is isotropic by (10), and is homogeneous.

As (39) is a generalized Riccati equation for β , it can be integrated. The general solution is,

$$e^{\beta(\rho,\tau)} = a(\tau) [C_1(\rho) + C_2(\rho)w(\tau)]^{2/3}, \quad \text{where } w(\tau) = \int_{\tau_0}^{\tau} \frac{dt}{a(t)^3}. \quad (40)$$

For this solution, we can compute that,

$$8\pi T_4^4 = 3 \left\{ \frac{\dot{a}}{a} + \frac{2C_2(\rho)\dot{w}}{3[C_1(\rho) + C_2(\rho)w]} \right\} \left\{ \frac{\dot{a}}{a} + \frac{2C_2'(\rho)\dot{w}}{3[C_1'(\rho) + C_2'(\rho)w]} \right\} \quad (41)$$

The dynamics of this model reveal that its predictions are at considerable variance with the observations of planetary astronomy. The slow-speed limit of the equations of motion follows directly from (29) and is, when we remember that $C_0 = O(c^{-1})$ in the slow speed limit,

$$\ddot{r} = \frac{\ddot{a}}{a}r - \frac{2C_2(\rho)^2}{9a^3r^2} - \frac{2\dot{a}C_2(\rho)r}{3a(ra)^{3/2}} + \frac{c^2C_0^2}{r^3}, \quad (42)$$

where $r(\rho, \tau) = e^{\beta(\rho, \tau)}$. In order to agree with Newton's result, we must choose $C_2(\rho) = -\frac{3}{2}\sqrt{2GM}$. The choice of $C_1(\rho)$ does not affect the dynamics, so we pick $C_1 = \frac{3}{2}\sqrt{2GM/c^2}\rho$. This choice suffices to cause $T_4^4 \rightarrow 3(\dot{a}/a)^2$ as $\rho \rightarrow \infty$. (Note that different choices of C_1 and C_2 are required for the zero mass case.)

This result is substantially unique for a model which has isotropic spatial curvature, a non-zero central mass concentration, and is asymptotic, at large distances from that mass, to the Friedmann-Lemaître, expanding universe model. However, this model leads, by (42), to the results,

$$\ddot{r} = \frac{\ddot{a}}{a}r + \frac{\dot{a}}{a^2}\sqrt{\frac{2GM}{ar}} - \frac{GM}{a^3r^2} + \frac{c^2C_0^2}{r^3}. \quad (43)$$

The problem to be noticed is the factor of a^3 in the denominator of the Newton gravitational attraction term. The import of this factor is that the radius of the earth's orbit will be proportional to a^3 as the gravitational term and the angular momentum term dominate the other terms. By Kepler's law that the ratio of the squares of the periods is proportional to the cube of the diameters, the year will be proportional to $a^{9/2}$. This means that the year should be increasing at the rate of about $0.73h_{50}$ seconds per century. Here h_{50} is the Hubble constant in units of 50 kilometers per second per Megaparsec. Since the value currently accepted by the International Astronomical Union is $+0.0095$ seconds per Julian century [17], the predictions of this model are in very serious disagreement with observations. The above results are in terms of the time variable τ . Properly done, we need the results in terms of time measured on the Earth for the Liebovitz line element. The re-expression of this result in terms of "Earth time" involves a correction of the order of $H_0GM_\odot/(c^2R_\oplus)$ where M_\odot is the mass of the Sun and r_\oplus is the radius of the orbit of the Earth. This quantity is of the order of 10^{-8} smaller than H_0 which is of the order of the predicted effect. Hence, this latter correction is negligible in this case. There is, of course, also a time independent correction to the relation between earth time and τ of the order of $GM_\odot/(c^2R_\oplus)$ but it is not relevant to the effect discussed here.

The conclusion of this section is that in one way or another, all the models reviewed that join the Schwarzschild metric at small distances and the expanding universe metric at large distances have problems of one sort or another. Panek [18] has stress the need to go beyond the "Swiss Cheese Model" and has analyzed numerically several different density profiles. In the next section, we will analyze the effect of a mass concentration inserted in a universe with a homogeneous mass-energy density.

4. HOMOGENEOUS, MASS-ENERGY DENSITY SOLUTIONS

In line with the idea that the vacuum has a homogeneous self-energy, we consider homogeneous mass-energy density solutions to Einstein's field equations. Our case of interest is the embedding of a mass concentration in expanding, curved space. We impose the condition,

$$\begin{aligned} 8\pi T_4^4 &= 3 \left(\frac{\dot{\beta}}{c} \right)^2 + 2 \frac{\dot{\beta}\dot{\beta}'}{c^2\beta'} + e^{-2\beta} \left[1 - f^2(\rho) - \frac{2f(\rho)f'(\rho)}{\beta'} \right] - \Lambda \\ &= 3 \left(\frac{\dot{a}}{ca} \right)^2 + \frac{3}{(aR_0)^2} - \Lambda \end{aligned} \quad (44)$$

which is the Friedmann-Lemaître value in curved space. Since the right hand side is a function of τ alone, we may integrate this equation, as at (15), with respect to ρ to give,

$$\dot{\beta}^2 + c^2 e^{-2\beta} [1 - f^2(\rho)] = \left(\frac{\dot{a}}{a} \right)^2 + \frac{c^2}{(aR_0)^2} + C_3(\tau) e^{-3\beta}. \quad (45)$$

At short distances, we wish to match the Lemaître-Schwarzschild metric (6). We find, upon substituting in (45), for $\dot{\beta}$ that

$$2GM e^{-3\beta} + c^2 e^{-2\beta} [1 - f^2(\rho)] \approx \left(\frac{\dot{a}}{a} \right)^2 + \frac{c^2}{(aR_0)^2} + C_3(\tau) e^{-3\beta}. \quad (46)$$

Thus, we shall choose $C_3(\tau) = 2GM$ independent of τ . For later convenience we rewrite (45) as

$$\dot{\beta}^2 = \left(\frac{\dot{a}}{a} \right)^2 + \frac{c^2}{(aR_0)^2} + 2GM e^{-3\beta} - c^2 e^{-2\beta} [1 - f^2(\rho)]. \quad (47)$$

If we are given $\beta(\rho_0, \tau_0)$, then this non-linear, first-order differential equation may be integrated with respect to τ to give $\beta(\rho_0, \tau) \forall \tau$.

In the special case $M = 0$ we have the Friedmann-Lemaître solution, and the special case, $\dot{a} = \ddot{a} = 0$, $R_0 = \infty$ gives us agreement with the Lemaître form of the static Schwarzschild metric (6).

Next we compute T_1^1 from (9) and the differentiation of (47). We obtain,

$$8\pi c^2 T_1^1 = 3 \left(\frac{\dot{a}}{a} \right)^2 + \frac{3c^2}{(aR_0)^2} \quad (48)$$

$$+ \frac{2 \left[\frac{\dot{a}\ddot{a}}{a^2} - \left(\frac{\dot{a}}{a} \right)^3 - \frac{\dot{a}c^2}{a^3 R_0^2} \right]}{\left\{ \left(\frac{\dot{a}}{a} \right)^2 + \frac{c^2}{(aR_0)^2} + 2GM e^{-3\beta} - c^2 e^{-2\beta} [1 - f^2(\rho)] \right\}^{1/2}}$$

which reduces correctly in the two special cases “flat space” with $\dot{a} = \ddot{a} = 0$, and $M = 0$. Since T_1^1 is not independent of ρ , the spatial curvature is neither homogeneous nor isotropic. It varies, as the distance from the mass concentration increases, from $3(\dot{a}/a)^2 + 3c^2/(aR_0)^2$ according to (48), to the Friedmann-Lemaître limit $2(\ddot{a}/a) + (\dot{a}/a)^2 + c^2/(aR_0)^2$ as the distance tends to infinity. The McVittie solution mentioned above has isotropic, but inhomogeneous, spatial curvature. The difference with this solution lies in the choice here that the universal expansion factor is a function of the proper time and his choice that it is a function of his coordinate time, which is not an invariant quantity.

So far, we have not had to discuss β' or $\dot{\beta}'$, as $\dot{\beta}$ given by (47) has sufficed for all our computations. The general equations do not determine the behavior of β as a function of ρ .

We observe that in the case of the expanding, curved-space of the Friedmann-Lemaître model universe, that

$$\frac{c^2}{(aR_0)^2} - c^2 e^{-2\beta} [1 - f^2(\rho)] = 0 \quad (49)$$

Since we wish our solution to tend asymptotically to this limit, we choose to require this result in the long distance limit. As a result of this consideration, we choose as initial conditions for (47)

$$\exp \beta(\rho, \tau_0) = R_0 \sin \left(\frac{\rho}{R_0} \right), \quad (50)$$

$$f(\rho) = \sqrt{1 - R_0^2 \sin^2 \left(\frac{\rho}{R_0} \right) / R_0^2}, \quad (51)$$

where, as the dependence on R_0 is actually a dependence on R_0^2 , there is no problem with the case where $R_0^2 < 0$. The continuation is just $x \sin(\rho/x) \mapsto |x| \sinh(\rho/|x|)$. Using these initial conditions and $a(\tau_0) = 1$ we find that (49) is exactly satisfied initially. In addition the ratio between the surface area of a sphere and the square of the radius is in accord with that for the Friedmann-Lemaître solution [5] for expanding, curved space in the open, closed, and “flat” cases. This choice, together with (47), defines $\beta \forall \rho, \tau$.

The dynamics are given by (29). The slow speed limit of the equation of motion is,

$$\ddot{r} = \left\{ \begin{array}{l} \left(\frac{\dot{a}}{a}\right)^2 + \frac{2 \left[\frac{\dot{a}\ddot{a}}{a^2} - \left(\frac{\dot{a}}{a}\right)^3 - \frac{\dot{a}c^2}{a^3 R_0^2} \right]}{\left[\left(\frac{\dot{a}}{a}\right)^2 + \frac{c^2}{(aR_0)^2} + \frac{2GM}{r^3} - \frac{c^2}{r^2} [1 - f^2(\rho)] \right]^{1/2}} \right\} r \\ - \frac{GM}{r^2} + \frac{c^2 C_0^2}{r^3}. \end{array} \right. \quad (52)$$

The curvature of space and the expansion of the universe contribute corrections of second order which are currently undetectable in the planetary motions of our solar system.

The solutions of this section have assumed that: (i) There is spherical symmetry about the mass-energy concentration. (ii) $T_1^4 = T_4^1 = 0$. (iii) T_4^4 is homogeneous as specified by (44), but may be time dependent. (iv) The metric matches in the short distance limit, the form of the Lemaître form of the static Schwarzschild metric corresponding to a mass-energy concentration of strength M . That is to say, the region in which the gravitational force is much greater than that of the expansion of the universe. (v) The metric matches the long distance form of the Friedmann-Lemaître metric. Under these assumptions, the solutions of this section is substantially unique, subject to the usual freedom involving changes of variables. This result is a parallel to Birkhoff's theorem[19], but involves a different class of models than the class he considered.

5. PROPERTIES OF THE HOMOGENEOUS, MASS-ENERGY DENSITY SOLUTIONS

It is convenient to make the change of variables,

$$e^{\beta(\rho,\tau)} = a(\tau)e^{\sigma(\rho,\tau)}. \quad (53)$$

Then (47) becomes,

$$\dot{\sigma}^2 + 2\frac{\dot{a}}{a}\dot{\sigma} = \frac{c^2}{(aR_0)^2} + 2GM e^{-3\beta} - c^2 e^{-2\beta} [1 - f^2(\rho)], \quad (54)$$

which may be solved by means of the quadratic formula to give

$$\dot{\sigma} = \frac{\dot{a}}{a} \pm \left[\left(\frac{\dot{a}}{a}\right)^2 + \frac{c^2}{(aR_0)^2} + \frac{2GM}{e^{3\beta}} - \frac{c^2 \dot{\rho}^2}{R_0^2 e^{2\beta}} \right]^{1/2}, \quad (55)$$

where I have chosen a simple reparameterization of (45-51), to wit,

$$\hat{\rho} = R_0 \sin\left(\frac{\rho}{R_0}\right) \quad (56)$$

so that (51) becomes,

$$f(\hat{\rho}) = \sqrt{1 - \hat{\rho}^2/R_0^2} \quad (57)$$

I choose as initial conditions for (55),

$$a(\tau_0) = 1.0, \quad \exp[\sigma(\hat{\rho}, \tau_0)] = \hat{\rho} \quad (58)$$

We may now check the special case, $M = 0$ and $R_0 = \infty$. As we expect $e^\beta = a(\tau)\hat{\rho}$, it follows that $\dot{\sigma} = 0$ for this case. That result in turn implies the minus sign in (55) as \dot{a} is known to be positive. Next we check the case where e^β is very small. The dominant terms in (55) are,

$$\dot{\sigma} = \pm \sqrt{\frac{2GM}{(a(\tau)e^\sigma)^3}}. \quad (59)$$

Integrating this equation with respect to τ yields,

$$\exp\left[\frac{3}{2}\sigma(\hat{\rho}, \tau)\right] - \exp\left[\frac{3}{2}\sigma(\hat{\rho}, \tau_0)\right] = \pm \frac{3}{2} \sqrt{\frac{2GM}{c^2}} c \int_{\tau_0}^{\tau} a^{-3/2}(t) dt \quad (60)$$

When we note that the integral in (60) is approximately $\tau - \tau_0$, and by use of (58), we get,

$$\exp\left[\frac{3}{2}\sigma(\hat{\rho}, \tau)\right] \approx \hat{\rho}^{3/2} \pm \frac{3}{2} \sqrt{\frac{2GM}{c^2}} c (\tau - \tau_0) \quad (61)$$

In order to match the Schwarzschild-Lemaître metric (6) for small e^β we must choose the minus sign in (61) and hence also in (55). From the examination of these special cases, we conclude in general (assuming that $\dot{a} \geq 0$) that (55) must always be taken as,

$$\dot{U} = \frac{3\dot{a}}{2a}U - \frac{3}{2} \left[\left(\frac{\dot{a}}{a}U\right)^2 + \frac{2GM}{a^3(\tau)} + \frac{c^2 \sqrt[3]{U^2}}{(a(\tau)R_0)^2} \left(\sqrt[3]{U^4} - \hat{\rho}^2\right) \right]^{1/2}, \quad (62)$$

where $U \equiv \exp(\frac{3}{2}\sigma)$.

It is worth pointing out that when $a \equiv 1.0$ that (62) subject to the initial conditions (57-58) gives the *static, curved-space solution* to the

Einstein field equations for a mass concentration in a vacuum. In this special case, $\beta(\rho, \tau) = \sigma(\rho, \tau)$ by (53). Eq. (62) becomes in this case,

$$\dot{U} = -\frac{3}{2} \left[2GM + \frac{c^2 \sqrt[3]{U^2}}{R_0^2} \left(\sqrt[3]{U^4} - \hat{\rho}^2 \right) \right]^{1/2}, \quad (63)$$

where here $U \equiv \exp(\frac{3}{2}\beta)$. The integration of this equation follows directly using the aforementioned initial conditions. $\alpha(\rho, \tau)$ follows by (8) and (57). By (44) and (48), we conclude that the $T_1^1 = T_2^2 = T_3^3 = 3/(8\pi R_0^2)$ and $8\pi T_4^4 = R_0^{-2}$, as expected in a curved-space vacuum.

The time when an observer at rest with respect to the coordinate system, *i.e.* a freely falling observer, arrives at the mass concentration, *i.e.*, when $e^\sigma = 0$ for a given $\hat{\rho}$ with initial conditions (58), is given by

$$\begin{aligned} U(\hat{\rho}, \tau_{\text{zero}}) - U(\hat{\rho}, \tau_0) &= -\hat{\rho}^{3/2} = \\ &= -\frac{3}{2} \int_{\tau_0}^{\tau_{\text{zero}}} dt \left\{ \left[\frac{2GM}{a^3(\tau)} + \left(\frac{\dot{a}}{a} U \right)^2 + \frac{c^2 \sqrt[3]{U^2}}{(a(\tau)R_0)^2} \left(\sqrt[3]{U^4} - \hat{\rho}^2 \right) \right]^{1/2} \right. \\ &\quad \left. - \frac{3\dot{a}}{2a} U \right\} \quad \tau_{\text{zero}} \approx \tau_0 + \frac{2\hat{\rho}^{3/2}}{3\sqrt{2GM}} \end{aligned} \quad (64)$$

by (61) and (62) Thus the physically allowed range of time is $0 \leq \tau \leq \tau_{\text{zero}}(\hat{\rho})$.

For numerical computations it is convenient to choose dimensionless quantities. I select,

$$\begin{aligned} \mathcal{T} &= H_0 \tau, \quad \mathcal{U} = \left(\frac{H_0}{c} \right)^{3/2} U, \quad \mathcal{M} = \frac{GMH_0}{c^3}, \quad \frac{\dot{\mathcal{A}}}{\mathcal{A}} = \frac{\dot{a}}{H_0 a}, \quad \mathcal{R} = \frac{H_0}{c} \hat{\rho}, \\ \mathbf{R}_0 &= \frac{H_0}{c} R_0. \end{aligned} \quad (65)$$

The initial conditions are $\mathcal{A}(T_0) = \dot{\mathcal{A}}(T_0)/\mathcal{A}(T_0) = 1$, $\mathcal{U}(R, T_0) = \mathcal{R}^{3/2}$, and $\mathcal{M}_\odot \approx 0.799 \times 10^{-23} h_{50}$. For reference, one astronomical unit is about $0.808 \times 10^{-15} h_{50}$ in our dimensionless units and a Megaparsec is about $1.67 \times 10^{-4} h_{50}$. Thus we may rewrite (62) as

$$\dot{\mathcal{U}} = \frac{3\dot{\mathcal{A}}}{2\mathcal{A}} \mathcal{U} - \frac{3}{2} \left[\left(\frac{\dot{\mathcal{A}}}{\mathcal{A}} \mathcal{U} \right)^2 + \frac{2\mathcal{M}}{\mathcal{A}^3(\mathcal{T})} + \frac{\sqrt[3]{\mathcal{U}^2}}{(\mathcal{A}(\mathcal{T})\mathbf{R}_0)^2} \left(\sqrt[3]{\mathcal{U}^4} - \mathcal{R}^2 \right) \right]^{1/2}, \quad (66)$$

I have integrated this equation by means of the Runge-Kutta method [20] adapted to double precision.

There are several special cases for the solution of equation (66). First, when e^β is large, the solution is just $e^\beta = \rho a(\tau)$, both for the case of “flat” and curved space. This solution is just what one expects for the case of expanding Friedmann-Lemaître expanding space. The quantity e^α is given by (57) and (8) which is, of course, different for “flat” and curved space. I illustrate the large e^β case, and the approach to it in fig. 2 for the case of flat space and $a(\tau) = (\tau/\tau_0)^{2/3}$. The initial conditions (58) insure that $e^\beta/[\hat{\rho}a(\tau_0)] = 1$ in every case. The central mass has been chosen to be that of the Sun.

The next special case is when e^β is small. In this case, in line with with the Lemaître form of the Schwarzschild metric, it is appropriate to plot the results vs. $(\tau - \tau_0)/\hat{\rho}^{3/2}$. This is because this form of the (static) metric can be written as

$$\frac{e^\beta}{\hat{\rho}} = \left[\frac{3}{2} \sqrt{\frac{2GM}{c^2}} \left(1 - \frac{c(\tau - \tau_0)}{\hat{\rho}^{3/2}} \right) \right]^{2/3} \quad (67)$$

I illustrate this case and the the approach to this limit in fig. 3. The large dots indicate the expected $[\hat{\rho} - c(\tau - \tau_0)]^{2/3}$ limiting curve with vertex at τ_{zero} .

The divergence at $\tau = 0$ noted in fig. 2, leads to the question of the nature of this divergence. It turns out that it depends on the exponent γ defined in the limit as $\tau \rightarrow 0$ by $a(\tau) \asymp W\tau^\gamma$. By considering the dominant terms in (66) for flat space, we obtain the results,

$$e^\beta \asymp \frac{c}{H_0} \left[\frac{2\mathcal{M}}{4(\gamma - \frac{1}{3})^2 - \gamma^2} \right]^{1/3} \left(\frac{\tau}{\tau_0} \right)^{2/3}, \quad \gamma > \frac{2}{3}, \quad (68)$$

$$e^\beta \asymp \frac{c}{H_0} \left(\frac{\tau}{\tau_0} \right)^\gamma \left[C_4^2(\rho) - \frac{3\mathcal{M}}{\gamma(2-3\gamma)} \tau^{2-3\gamma} \right]^{1/3}, \quad 0 < \gamma < \frac{2}{3} \quad (69)$$

$$e^\beta \asymp \frac{c}{H_0} \left[-\frac{9}{2} \mathcal{M} \left(\frac{\tau}{\tau_0} \right)^2 \ln \left(\frac{\tau}{\tau_0} \right) \right]^{1/3}, \quad \gamma = \frac{2}{3}. \quad (70)$$

The behavior for values of γ not illustrated is qualitatively similar, but differs, of course, in detail.

The effects of the curvature of space on β is not very significant either for small values of e^β or for large values, as in these cases the limiting values discussed above are obtained. The effects however are of some significance for intermediate values of e^β . I have illustrated an example in fig. 4.

6. DOMAINS OF ATTRACTION

In this section we will focus our attention on the slow-speed (52), flat-space[1, 2] limit of (29) for radial motion only. That is to say, $C_0 = 0$. Hence, using the dimensionless variables of (65), we obtain,

$$\ddot{\mathfrak{R}} = \left(\frac{\dot{\mathcal{A}}}{\mathcal{A}}\right)^2 \mathfrak{R} + \frac{\left[\frac{\dot{\mathcal{A}}\ddot{\mathcal{A}}}{\mathcal{A}^2} - \left(\frac{\dot{\mathcal{A}}}{\mathcal{A}}\right)^3\right] \mathfrak{R}}{\left[\left(\frac{\dot{\mathcal{A}}}{\mathcal{A}}\right)^2 + \frac{2\mathcal{M}}{\mathfrak{R}^3}\right]^{1/2}} - \frac{\mathcal{M}}{\mathfrak{R}^2} \quad (71)$$

where $\mathfrak{R} = H_0 e^\beta / c$. First consider the case where the rate of expansion of the universe is decreasing. Then $\dot{\mathcal{A}} < 0$. If we divide (71) by $(\dot{\mathcal{A}}/\mathcal{A})^2 \mathfrak{R}$ and let $x = \mathcal{M}A^2/(\mathfrak{R}^3 \dot{\mathcal{A}}^2)$, then it becomes

$$\left(\frac{\mathcal{A}}{\dot{\mathcal{A}}}\right)^2 \frac{\ddot{\mathfrak{R}}}{\mathfrak{R}} = 1 - x - \frac{1}{\sqrt{1+2x}} + \frac{\ddot{\mathcal{A}}\mathcal{A}}{\dot{\mathcal{A}}^2 \sqrt{1+2x}} \quad (72)$$

Note that the $\ddot{\mathcal{A}}$ term in (72) is uniformly negative over the allowed range of x , ($0 \leq x \leq \infty$). Hence we may check all the cases $\dot{\mathcal{A}} \leq 0$ by setting it to zero. This being done, we may compute in a straight forward manner that for very small x , the right-hand side is just $-1.5x^2$. Differentiation with respect to x shows that the derivative is uniformly negative. Thus we conclude that if the rate of expansion of the universe is not increasing, then according to the metric of found in section IV, there is just one domain of attraction and it is centered on the mass concentration as (72) shows that if $\dot{\mathcal{A}} \leq 0$, then $\ddot{\mathfrak{R}} < 0$. The analogous computations for curved space proceed in a similar manner, but are a bit more complicated.

Next let us consider the case where, as reported by Reiss *et al.*[3] and Perlmutter *et al.*[4], the rate of expansion of the universe is increasing. As for this case, $\dot{\mathcal{A}} > 0$, it follows directly from (71) that in the limit as $\mathfrak{R} \rightarrow \infty$, $\ddot{\mathfrak{R}} > 0$. Since it is also the case that when $\mathfrak{R} \rightarrow 0$, $\ddot{\mathfrak{R}} < 0$, it follows that there exists an \mathfrak{R}_D for which $\ddot{\mathfrak{R}} = 0$. Therefore, we now have two domains of attraction. One is $0 \leq \mathfrak{R} < \mathfrak{R}_D$. In this domain, all test particles at rest with respect to the coordinate system appear to be accelerating towards the origin. The other domain is $\mathfrak{R}_D < \mathfrak{R}$. In this domain all test particles at rest with respect to the coordinate system appear to be accelerating towards infinity. One expects that over time, the neighborhood of the domain boundary will be swept clean of particles.

Note is taken that the “Swiss cheese model” also has 2 domains of attraction. This fact is independent of the sign of \ddot{a} . Also the location of the boundary described by \mathfrak{R} increases with time.

At this point it is convenient to define the standard acceleration/deceleration parameter $q_0 \equiv -\ddot{A}/(\dot{A}^2)$. Then, setting $\ddot{\mathfrak{R}} = 0$, the equation for the domain boundary becomes, by (72),

$$0 = 1 - x - \frac{q_0 + 1}{\sqrt{1 + 2x}} \quad (73)$$

The value of q_0 is given[21] by the equation,

$$q_0 = \frac{1}{2}\Omega_M - \Omega_\Lambda \quad (74)$$

where, combining the results of [1, 2, 3, 4] we deduce the values $\Omega_M = 8\pi G\rho_0/(3H_0^2) \approx 0.19$ and $\Omega_\Lambda = \Lambda c^2/(3H_0^2) \approx 0.81$. These values yield $q_0 \approx -0.715$. Note that for “flat” space, $-1 \leq q_0$, as $0 \leq \Omega_M$. Some simple manipulations convert (73) into a cubic equation in x .

$$2x_D^3 - 3x_D^2 + 1 = (1 + q_0)^2 \quad (75)$$

This equation is simply solved by standard methods. Its solutions, of course, also include those for the other sign of the square root in (73). Evidently, the solutions of (73) all lie in the range $0 \leq x \leq 1$. If $q_0 \geq 0$, there are no positive real roots of (73) and we take $x_D(q_0) = 0$. If $q_0 < 0$, then there is one positive real solution $x_D(q_0)$ of (73). For the above mentioned case, $x_D(-0.715) \approx 0.825$.

We now have the *domain-size-mass relation*,

$$r_D = \left[\frac{GMa^2}{x_D(q_0)\dot{a}^2} \right]^{\frac{1}{3}}. \quad (76)$$

Here r_D is the radius of the domain and M is the interior mass. We appeal to the uniqueness (in our class of models) reported at the end of the fourth section to allow us to treat all the mass as concentrated in the center of the domain. See also the result (16) in this regard. The *domain-size-mass relation* is an important conclusion which is of particular interest if the rate of expansion of the universe is accelerating, as has recently been reported[3, 4].

It is to be noted that many mass concentrations are rotating and so are only axisymmetric, rather than spherically symmetric. This means that near the mass concentration the metric has some of the characteristics of the Kerr metric. In terms of Cartesian coordinates, the differences in the far-field between the Kerr metric and the Schwarzschild metric [8] are $g_{4i} \simeq 2G(\vec{r} \times \vec{I} \cdot \vec{e}_i)/(rc)^3$, where the \vec{e}_i are unit vectors

in the x , y , z directions and \vec{I} is the angular momentum of the central mass concentration. In regions where this correction is relatively small compared to the gravitation term $2GM/(c^2r)$, *i.e.*, $|\vec{r} \times \vec{I}|/(Mc^2r^2) \ll 1$, we may safely neglect this effect. On the other hand, where the correction is significant, the precise details of this effect will require further study. In addition, our lack of a clear knowledge of the distribution of dark matter also creates uncertainty concerning the details the above obtained results.

We now consider a few applications of the *domain-size-mass relation*. If we use the solar mass, we get the radius of the domain boundary to be about $417h_{50}^{-2/3}$ light years. However, in this case the density of stars is sufficiently high so as to perturb significantly this result. The Oort cloud only extends out to about 0.8 light years. We remark that the *domain-size-mass relation* only provides an upper limit on the size of a structure that a given mass can be expected to hold together. That there are smaller structures can presumably be explained on the basis of other circumstances.

Next consider a globular cluster. They are observed to have about 10,000 to 1,000,000 stars and to have diameters of several 10's of light years to about 200 light years. The computed domain boundary diameters for systems of this size are about $9000h_{50}^{-2/3}$ - $42000h_{50}^{-2/3}$ light years. This result is of the substantially larger than that which is observed. It may be that they are reduced in size when they orbit near the galactic center.

Let us now consider our galaxy. It is estimated to contain something like 200 billion stars and to have a mass of 700 billion to 1 trillion solar masses. This mass implies a domain radius of $3.7h_{50}^{-2/3}$ to $4.2h_{50}^{-2/3}$ million light years, which way off from the observationally estimated diameter of about 100 thousand light years.

When we consider the Local Group and the Virgo Cluster, the problem becomes more interesting. Specifically, it has been estimated that the roughly 30 galaxies in the local group have a mass of about $3 \times 10^{12}M_{\odot}$, not counting intergalactic dark matter. This mass corresponds to about a radius of $6h_{50}^{-2/3}$ million light years. The observed value is roughly 4 million light years. In the Virgo Cluster of around 2000 galaxies, the mass is thought to be of the order of $10^{15}M_{\odot}$. This mass includes a significant amount of dark matter and gives a radius of about $42h_{50}^{-2/3}$ million light years, compared to the observation that the Milky Way galaxy lies about 65 million light years from center of the cluster. Considering the errors and the fact that the Virgo Cluster appears not to be in equilibrium yet, this agreement is not too bad.

In conclusion, it appears that for larger scale structures composed of galaxies and inter-galactic space, the observed increase in the rate of expansion may be an important feature in determining the size of self-bound gravitating systems. For smaller structures like galaxies, globular clusters *etc.* other mechanisms are presumably dominant.

Acknowledgements

The author is pleased to acknowledge helpful conversations with N. Balazs, S. Habib, P. O. Mazur, E. Motolla, and M. M. Nieto.

References

1. P. de Bernardis, P. A. R. Ade, J. J. Bock, J. R. Bond, J. Borrill, A. Boscaleri, K. Coble, B. P. Crill, G. de Gasperis, P. C. Farese, P. G. Ferreira, K. Ganga, M. Giacometti, E. Hivon, V. V. Hristov, A. Iacoangeli, A. H. Jaffe, A. E. Lange, L. Martinis, S. Masi, P. V. Mason, P. D. Mauskopf, A. Melchiorri, L. Miglio, T. Montroy, C. B. Netterfield, E. Pascale, F. Piacentini, D. Pogosyan, S. Prunet, S. Rao, G. Romeo, J. E. Ruhl, F. Scaramuzzi, D. Sforna, and V. Vittorio, *Nature*, **404**, 955 (27 April 2000).
2. W. Hu, *Nature* **404**, 939 (27 April 2000).
3. A. G. Reiss, A. V. Filippenko, P. Challis, A. Clocchiatti, A. Diercks, P. M. Garnavich, R. L. Gilliland, C. J. Hogan, S. Jha, R. P. Kirshner, B. Leibundgut, M. M. Phillips, D. Reiss, B. P. Schmidt, R. A. Schommer, R. C. Smith, J. Spyromilio, C. Stubbs, N. B. Suntzeff, and J. Tonry, *Astron. J.* **116**, 1009 (1998). xxx.lanl.gov, astro-ph/9805201.
4. S. Perlmutter, G. Aldering, G. Goldhaber, R. A. Knop, P. Nugent, P. G. Castro, S. Deustua, S. Fabbro, A. Goobar, D. E. Groom, I. M. Hook, A. G. Kim, M. Y. Kim, J. C. Lee, N. J. Nunes, R. Pain, C. R. Pennypacker, R. Quimby, C. Lidman, R. S. Ellis, M. Irwin, R. G. McMahon, P. Ruiz-Lapuente, N. Walton, B. Schaefer, B. J. Boyle, A. V. Filippenko, T. Matheson, A. S. Fruchter, N. Panagia, N. J. M. Newburg, and W. J. Couch, *Astrophys. J.* **517**, 565 (1999). xxx.lanl.gov, astro-ph/9812133.
5. P. J. E. Peebles, *Principles of Physical Cosmology* (Princeton University Press, Princeton, NJ, 1993).
6. G. Lemaître, *Ann. de la Soc. Scient. de Bruxelles* **A53**, 51 (1933).
7. R. C. Tolman, *Proc. Nat. Acad. Sci. USA* **20**, 169 (1934).
8. H. Stephani, *General Relativity (second edition)*, (Cambridge Univ. Press, 1990, New York).
9. G. Lemaître, *Comp. Rend. Acad. Sci. (Paris)* **196**, 903 (1933).
10. A. Krasiński, *Inhomogeneous Cosmological Models* (Cambridge Univ. Press, 1997, Cambridge).
11. G. C. McVittie, *M. N. R. A. S.*, **93**, 325 (1933).
12. A. Einstein and E. G. Straus, *Rev. Mod. Phys.* **17**, 120 (1945); erratum **18**, 148 (1946).

13. H. Sato, in *General Relativity and Gravitation*, B. Bertotti, F. de Felice, and A. Pascolini, eds. (Reidel, 1984, Dordrecht), pg. 289.
14. K. Lake and R. Pim, *Astrophys. J.* **298**, 439 (1985).
15. C. Bona and J. Stela, *Phys. Rev. D* **36**, 2915 (1987).
16. C. Liebovitz, *Phys. Rev. D* **4**, 2949 (1971).
17. J. Q. Jacobs on the world wide web at
<http://www.geocities.com/Athena/Olympus/4844/astrofor.htm>
18. M. Panek, *Astrophys. J.* **388**, 225 (1992).
19. G. D. Birkhoff, *Relativity and Modern Physics* (Harvard University Press, Cambridge, Mass., 1923)
20. W. H. Press, S. A. Teukolsky, W. T. Vetterling, and B. P. Flannery, *Numerical Recipes in Fortran; The Art of Scientific Computing*, second edition (Cambridge Univ. Press, Cambridge, 1992).
21. See for example, S. M. Carroll, W. H. Press, and E. L. Turner, *Annual Rev. Astron. Astrophys.* **30**, 499 (1992).

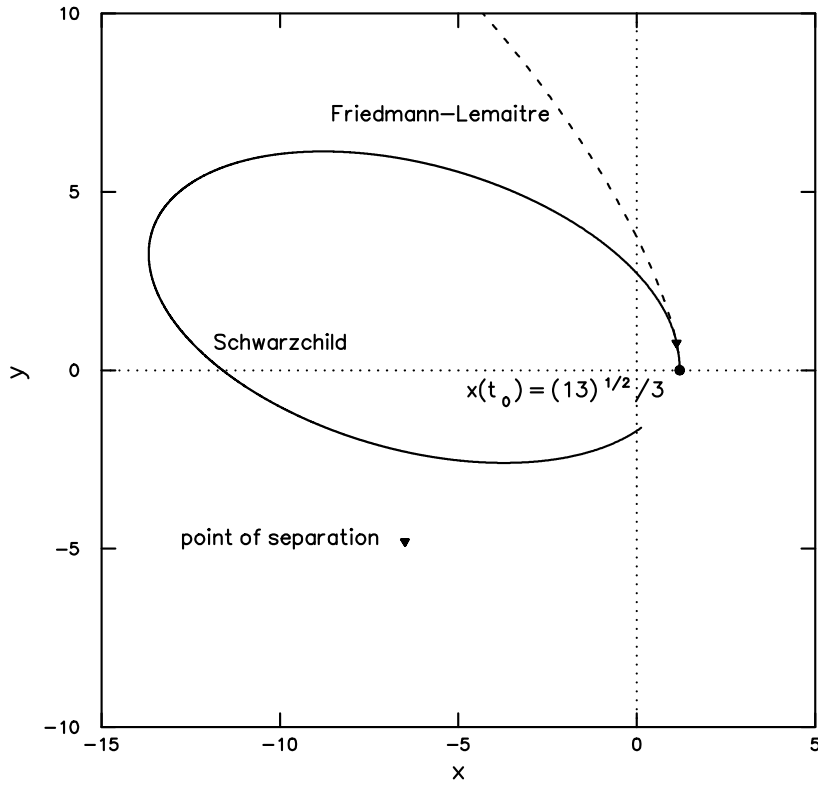


Figure 1. “Swiss cheese model” trajectories which begin at $x_0 = \sqrt{13}/3 + \epsilon$ (the Friedman-Lemaître case), and begin at $x_0 = \sqrt{13}/3 - \epsilon$ (the Schwarzschild case). Here, $\epsilon > 0$ may be chosen as small as one pleases. The initial part of both trajectories is a parabola generated by the Friedmann-Lemaître metric. At time $t = (13/11)^3$, marked in the figure, the two trajectories separate.

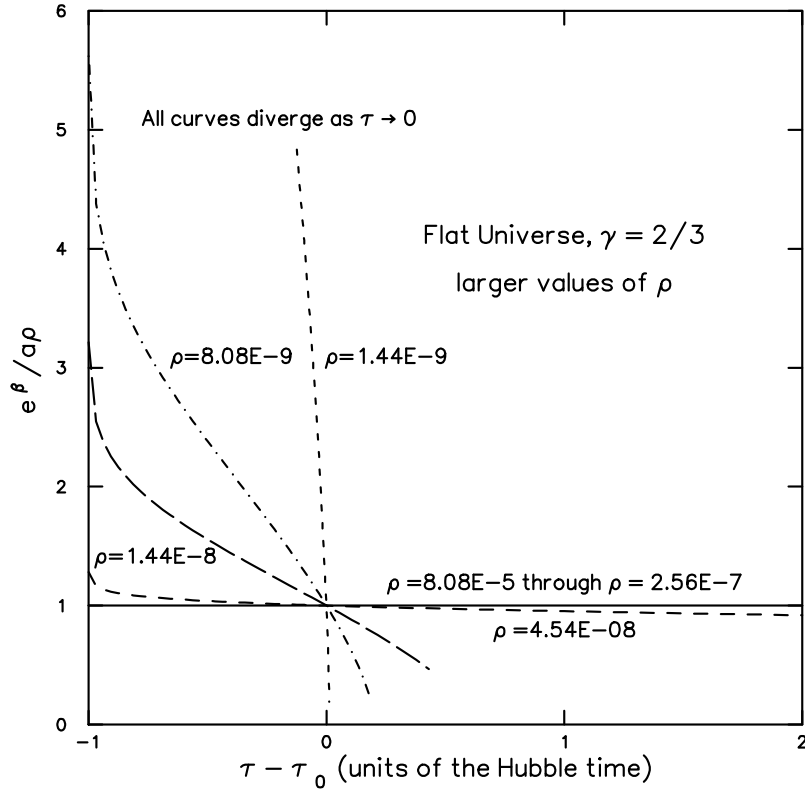


Figure 2. The behavior of $e^{\beta(\rho, \tau)}$ for larger values of ρ . The solid line is the limiting value obtained for large values of ρ . It is $e^\beta = a(\tau)\rho$. The other lines show how the limit is approached as ρ increases.

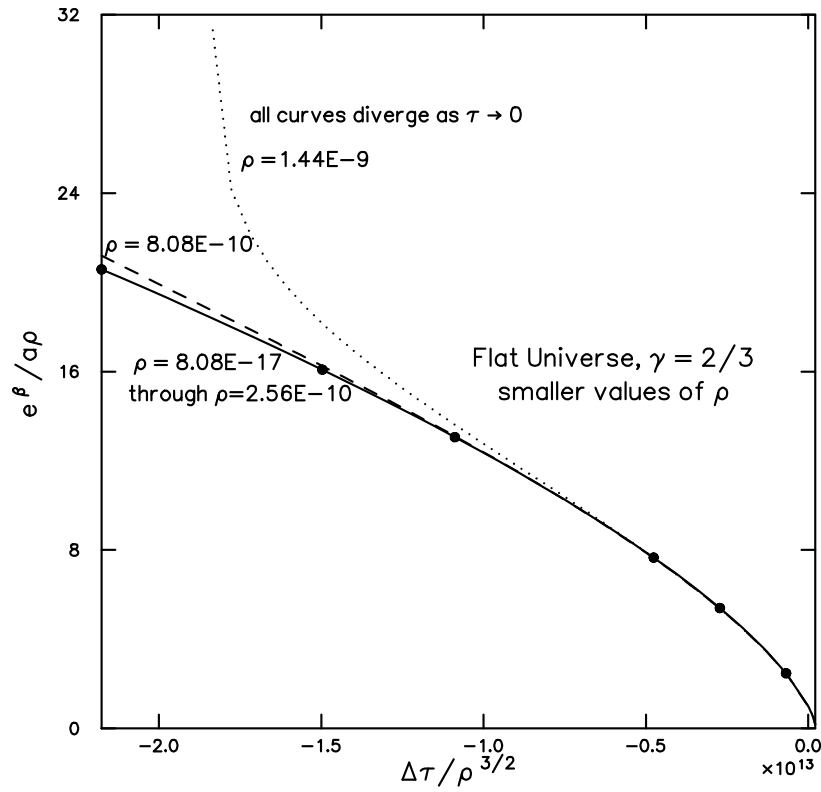


Figure 3. The behavior of $e^{\beta(\rho, \tau)}$ for smaller values of ρ . The solid line is the limiting value obtained for smaller values of ρ . It is $e^\beta \propto a(\tau)\rho[1 - c(\tau - \tau_{\text{zero}})/\rho^{3/2}]^{2/3}$. The large dots show this formula. The other lines show how the limit is approached as ρ decreases.

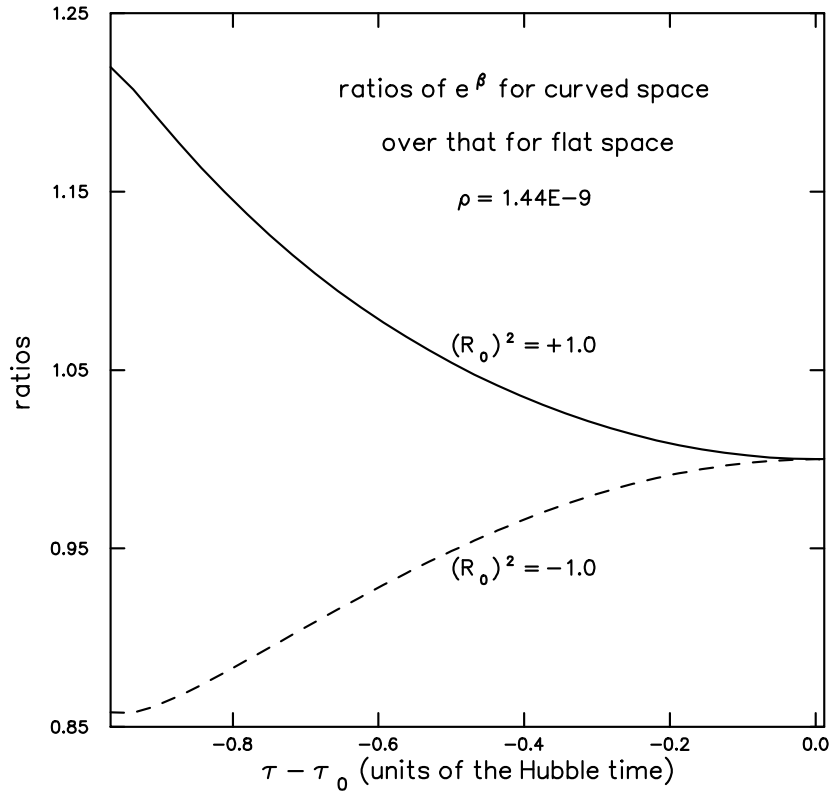


Figure 4. The variation of $e^{\beta(\rho,\tau)}$ with the curvature of space. Displayed are the ratios of e^β for curved space to that for “flat” space with the same values of ρ, τ . The solid curve is for $R_0^2 = +1$ and the dashed curve is for $R_0^2 = -1$.

